Proceedings of the 17th World Congress
The International Federation of Automatic Control
Seoul, Korea, July 6-11, 2008

Review of Feedforward Approaches for Nano Precision Positioning in High Speed SPM Operation

Santosh Devasia *

* *Mechanical Engineering Department, U. of Washington, Seattle, WA 98195, USA (Tel: 206-685-3401; e-mail: devasia@u.washington.edu).*

Abstract: This article reviews developments in feedforward control for Scanning Probe Microscopes (SPMs), which are key enabling tools in nanotechnologies. Feedforward control aids in precision positioning (at the nano scale) needed to achieve the current research goal of increasing SPM's operating speed.

1. INTRODUCTION

Precision positioning is critical in Scanning Probe Microscopes (SPMs) such as scanning tunneling microscopes (STMs [1]) and Atomic Force Microscopes (AFMs [2]). This article reviews the control problems and approaches in current SPMs. While both feedback and feedforward are important in achieving precision positioning, this article focuses on feedforward control techniques; feedback control is the focus of two other keynote articles in this series of invited sessions, e.g. [3, 4] and is also discussed in a recent review on nano-precision positioning [5]. Moreover, this article discusses the integration of feedforward with sensor-based feedback, as well as the image-based approach to feedforward control that does not require additional sensors other than the standard SPM-probe sensor such as the AFM-probe-deflection sensor.

1.1 AFM Operation

Precision positioning is important in each of the large family of SPMs, which measure a variety of surface properties such as chemical, mechanical, electric and magnetic properties, e.g., [6]. In the following, the article emphasizes AFM operation; the control issues are similar in other SPMs. For example, during AFM imaging, a piezoscanner (based on piezoelectric actuators) changes the position of the AFM probe (tip of an AFM-cantilever) relative to the sample surface, as shown in Fig. 1. Other possible positioning schemes including the sample being moved rather than the AFM probe and the use of separate/multiple stages for different axes.

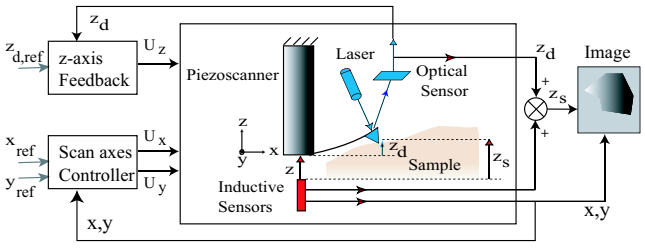

Fig. 1. AFM-probe positioning using a piezoscanner in the lateral scan x-y and vertical z axes.

The force between the AFM probe and the sample surface is controlled using a feedback loop when scanning the sample surface, as follows. First, the applied tip-sample force is estimated by measuring the deflection z_d of the AFM probe [7]. Second, the measured AFM-probe deflection is used in a feedback loop to apply an input U_z that adjusts the vertical position z of the piezoscanner and maintains the AFM-probe deflection z_d at the desired value $z_{d,ref}$. An AFM image of the sample is obtained, for example, by plotting (a) the vertical position z_s of the AFM-probe's tip over the sample against (b) the lateral position x-y.

1.2 Need for Precision Positioning Control

Broadly, two types of positioning are needed: (i) lateral positioning in the scan axes x-y; and (ii) vertical positioning along the z axis.

Lateral x-y Positioning: Lateral precision is important when manipulating/modifying a specific location on the sample surface. For example, the probe needs to move along a specified scan trajectory x_{ref}-y_{ref} (see Fig. 1) where surface alteration is desired during nanofabrication [8]. Lateral positioning errors lead to distortions of the achieved nano-scale features.

It is noted that lateral precision is not as critical during routine imaging applications because the x-y position can be measured and used to plot the images — rather than using the reference trajectories x_{ref}-y_{ref} to plot the image, which was common practice before the use of sensors to measure the lateral x-y position.

Vertical z Positioning: Vertical positioning is critical during, both, imaging and modification. For example, during AFM imaging, the vertical position z affects the AFM-probe deflection z_d, and thereby, affects the tip-sample force, i.e, the force between the AFM-probe's tip and the sample surface. Ideally, if the AFM probe's position z_s precisely follows the sample's topography (i.e., the sample profile along each scan line as shown in Fig. 2), then the AFM probe deflection (and the tip-sample force) can be zero. However, in practice a small tip-sample force is needed to maintain contact between the AFM probe and the sample in the presence of vibrational noise.

Nevertheless, it is important to track the sample profile, because if the probe does not follow the sample profile, then the resulting excessive tip-sample force can cause large sample deformation in soft samples (sample surface is then substantially different from the AFM probe position z_s), as well as sample modification and possibly sample damage.

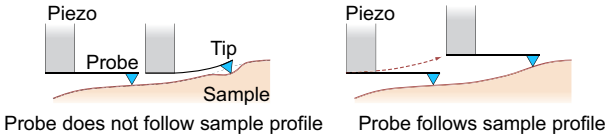

Fig. 2. Precision vertical positioning allows the AFM-probe to follow the sample profile along each scan line without excessive probe deflection, and thereby, to maintain a small tip-sample force.

When imaging relatively hard samples, damage is not a significant concern and therefore, higher scan frequencies are possible [9]; however, vertical positioning to track the sample profile is still important since excessive tip-sample force can damage the AFM probe. Thus, precision positioning in the vertical axis is needed to maintain a small AFM-probe deflection z_d and thereby, to maintain a small tip-sample force during AFM operation.

Vertical positioning is also critical when modifying the surface. For example, nano-scale parts can be fabricated by using the AFM probe as an electrode to induce local-oxidation by applying a voltage between the AFM probe and the surface, e.g., [10]. The vertical position of the AFM probe with respect to the sample has a dominant effect on the applied current and the formation of the current-induced oxide [11]. Therefore, precision vertical positioning is important to avoid distortion in the size and shape of the nanofabricated parts.

1.3 Need for High-Speed SPM

High-speed SPM operation is desirable for, both, the imaging and manipulation of nanoscale phenomena.

High-Speed Imaging: SPM images will be substantially distorted if the surface property being investigated is changing rapidly in time (in comparison to SPM's operating speed) because measurements at the initial pixel and at the final pixel of an image are acquired at different times as the SPM-probe is scanned over the sample. Therefore, there is a need to develop high-speed SPM to study, manipulate, and control of processes with fast dynamics. For example, increases in SPM's operating speed will advance the discovery and understanding of dynamic phenomena by enabling: (a) the study of rapid melting and crystallization of polymers (e.g., [12]-[14]); (b) the investigation of fast phase transitions in ferroelectric materials (e.g., [15]) that influences domain formation, which in turn affects physical properties (e.g., piezo-electricity, electro-optical properties, and hysteresis); and (c) single-molecule vibrational and force spectroscopy to elucidate structural and electronic information (e.g., [16, 17]).

High-Speed Nanofabrication: The main advantage of SPM-based nanofabrication is that it achieves the smallest features [8]. Unfortunately, SPM-based nanofabrication suffers from throughput limitations present in all serial techniques — the tip must visit each point where something is to be done. Even with multiple probes [18, 19] such serial processes cannot compete with parallel techniques like current optical lithography, which can process an entire wafer (more precisely, one die) in one step. One solution to the low-throughput problem is to integrate the slower, top-down, SPM nanofabrication with faster, bottom-up, nanofabrication methods. For example, rather than adding all the required material in a direct write approach, STM-based chemical vapor deposition (CVD) might be used only for *seeding* or prenucleating the desired pattern, whereas the rest of the material can then be grown by selective CVD [20]. Similarly, patterned self-assembled monolayers can be fabricated with AFM-based dip-pen nanolithography, which can then be used for nucleation and growth of functional polymers [21, 22]. In this sense, the top-down SPM is only needed for generating the initial pattern, which then forms the basis for growing the nanostructure using highly-parallel bottom-up techniques [23, 24]. High-speed SPM operation is desirable to increase the throughput of generating these initial seed patterns.

1.4 Precision Positioning is Critical to High-speed SPM

High-speed operation requires precision lateral positioning along the scan axes at higher frequencies, e.g., during nanofabrication. Moreover, as the scan frequency increases, the SPM-probe's tip has to track the sample's topography (i.e., sample profile in each scan line) faster for both imaging and manipulation. In either case, high-speed, precision positioning (lateral and/or vertical) is critical to high-speed operation. However, as the scan frequency is increased relative to the smallest, resonant-vibrational frequency of the piezoscanner, the vibrational modes of the piezoscanner are excited and the resulting vibrations cause positioning errors. Such positioning errors are different from those caused by vibrations transmitted to the SPM from external sources; external vibration problems can be relatively-easily addressed using vibration-isolation schemes, e.g., [25]. The positioning errors become significant at high scan frequencies; thereby, SPM-probe positioning errors limit the maximum SPM operating speed [26].

1.5 Approaches to Achieve High-Speed SPM

Two current approaches to achieve high-speed SPM operation are: (i) suppress vibration by flattening the frequency response; and (ii) increase the piezoscanner's bandwidth by increasing its resonant-vibrational frequency as illustrated in Fig. 3.

Approach i — Feedback to Suppress Vibration: Feedback control has been an integral part of SPM development; for example, integral controllers are very effective in maintaining the desired probe-sample interaction, e.g., the desired level of tunneling current in STM or the tip-sample force in AFM. Integral controllers are particularly effective during low-speed operation; they can overcome both creep and hysteresis effects (in the piezoscanners) and lead

to precision positioning (since the vibrational dynamics is not dominant at low frequencies). In this sense, traditional proportional-integral-derivative (PID) feedback controllers or a double integral for tracking a ramp, are well suited for nanopositioning and are popular in SPM applications [26]. Recent works have aimed to robustify such existing integral controllers in SPMs [27]. Essentially, feedback increases the positioning bandwidth by *flattening the frequency response* of the closed-loop piezoscanner in the region that contains the desired position-trajectory's frequency content.

The main challenge in feedback design is performance improvement while maintaining the stability of the overall system in the presence of parameter uncertainty and unmodeled high-frequency dynamics. Therefore, advanced control techniques have been applied to improve the precision and bandwidth of piezoscanners; see Ref. [5] for a review of such precision positioning approaches. In particular, starting with the early work in Ref. [28], modern feedback control techniques, e.g. [29]-[31], have enabled an increase in the operating speed of SPMs.

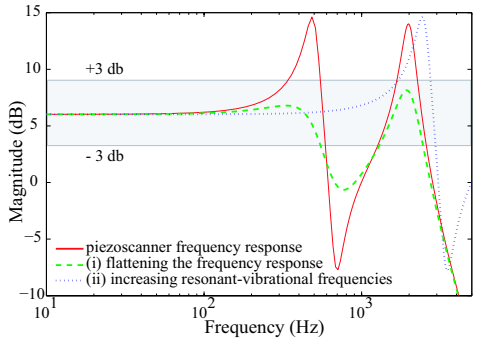

Fig. 3. Increasing bandwidth of piezoscanner by: (i) flattening the frequency response; and (ii) increasing the smallest resonant-vibrational frequency.

Approach ii — Increase Resonant-Vibrational Frequencies: Another approach to reduce vibration-caused positioning error is to use higher-bandwidth piezos in the piezoscanner, as shown in Fig. 3. Higher bandwidth implies that the piezoscanner's smallest, resonant-vibrational frequency is larger. Therefore, the frequency response of the piezoscanner is flat near the desired trajectory's (relatively lower) frequencies. Therefore, the positioning movement does not induce vibrations and the piezoscanner position matches the desired reference position. Thus, the use of high-bandwidth piezos allows higher operating speeds [9].

High-bandwidth piezoscanners can be developed by using short piezo-tubes or piezo-plates [32]. Similarly, miniaturized AFMs [19, 33, 34]) also increase the operating bandwidth because the resonant vibrational frequencies of smaller piezos tend to be higher. Such high-bandwidth piezoscanners have been used to visualize fast dynamic changes on surfaces using the AFM. For example, high-speed images of DNA plasmid movements have been obtained in Ref. [35]; the imaging time was $4s$ per image. More recently, a similar approach was used in Ref. [34] to enable AFM imaging at a high scan frequency of $1.25KHz$ and an imaging time of 80 milliseconds per frame.

Feedforward vs. Other High-Speed Approaches: The use of feedforward to reduce vibrational effects, and thereby to increase the operating speed of SPMs was first demonstrated in Ref. [36]. It is noted that the use of feedforward inputs can improve the positioning performance when compared with the use of feedback alone, even in the presence of plant uncertainties. The size of acceptable uncertainties, to guarantee that performance can only get better by adding feedforward to feedback, has been quantified in [37]. Similarly, feedforward can improve the performance of high-bandwidth piezoscanners because vibrations cause positioning errors even in high-bandwidth piezoscanners. Thus, feedforward can be used in conjunction with other methods, such as feedback and design of the positioning system to increase the resonant-vibrational frequencies, to further increasing SPM's operating speed.

2. FEEDFORWARD APPROACH

The difficulty in precisely positioning the SPM probe does not arise because the SPM probe cannot be moved by the piezoscanner at high scan frequencies. (*Piezoscanners tend to have low damping and therefore the SPM probe moves over a large scan area when the scan frequency is high, especially, when the scan frequency is close to the piezoscanner's resonant-vibrational frequencies.*) Rather, the problem is the lack of precision at positioning frequencies that are close to the piezoscanner's resonant-vibrational frequencies. This section reviews the use of the inversion-based approach [38, 39] to find feedforward inputs to the piezoscanner that enable precision positioning of the SPM probe.

2.1 Inversion-based Feedforward

The use of feedforward control to increase SPM's operating speed was demonstrated in [36], where the input voltage V applied to the piezoscanner was related to the output position P using Fourier transforms as

$$P(j\omega) \ = G(j\omega)V(j\omega) \tag{1}$$

Inverting the Vibrational Dynamics: The central idea of the inversion approach is to find the input voltage V_{inv} that when applied to the piezoscanner results in a desired position $P = P_d$. In particular, for a desired output position P_d, the piezoscanner input V_{inv} can be found by inverting the vibrational dynamics G using the approach by Bayo in [38]

$$V_{inv}(j\omega) \ = G^{-1}(j\omega)P_d(j\omega). \tag{2}$$

The time domain inverse input V_{inv} is then obtained using the inverse Fourier transform. If the piezoscanner dynamics is stable (i.e., G is stable), then the SPM probe can be positioned at the desired location P_d by applying this inverse input V_{inv} to the piezo-scanner.

Remark 1. Typical inverse inputs are unbounded for non-minimum phase systems, e.g.,when the zeros of G (which become the poles of G^{-1}) are on the right half of the complex plane. The computation of the inverse, using the Fourier transform and its inverse Fourier transform, results in bounded inputs V_{inv} even if the system G is nonminimum phase [38]. Therefore, this approach is referred to as the stable inversion approach.

Optimal Inverse: The optimal inverse developed in [40], an extension of the inverse (Eq. 2), allows for tradeoffs between the input size and the precision-positioning requirement at different frequencies. In particular, the optimal inverse input is found by minimizing the following cost function:

$$J(u) = \int_{-\infty}^{\infty} \{V^*(j\omega)R(j\omega)V(j\omega) + E_P^*(j\omega)Q(j\omega)E_P(j\omega)\}d\omega, \quad (3)$$

where $*$ denotes the complex conjugate transpose and $E_P = P - P_d$ is the positioning error. The terms $R(j\omega)$ and $Q(j\omega)$ are real-valued, frequency-dependent weightings that penalize the size of the input V and the positioning error E_P.

Remark 2. The optimal inverse input V_{opt} enables precise positioning ($P(j\omega) = P_d(j\omega)$) at a frequency ω by choosing a nonzero positioning-error weight $Q(j\omega) > 0$ and zero input weight $R(j\omega) = 0$. The other extreme in the choice of weights is when the input weight is nonzero $R(j\omega) > 0$ and the positioning-error weight is zero $Q(j\omega) = 0$. Then the cost function is minimal for not using any input at all, i.e., $V(j\omega) = 0$ at that particular frequency.

The optimal inverse input V_{opt} that minimizes the cost function (in Eq. 3) can be found as [40]

$$V_{opt}(j\omega) = \left[\frac{G^*(j\omega)Q(j\omega)}{R(j\omega) + G^*(j\omega)Q(j\omega)G(j\omega)}\right] P_d(j\omega) \quad (4)$$

and the time-domain signal for the feedforward input $V_{ff}(t)$ is then obtained through an inverse Fourier transform of $V_{opt}(j\omega)$.

Remark 3. The optimal inverse can be used to find feedforward inputs for actuator redundant systems such as multiple-stage positioners [41].

Application to SPM: The optimal inverse was applied to an STM in [36]. Fig. 4 shows the STM image of a highly oriented pyrolytic graphite (HOPG) surface. The uniform lattice pattern of the HOPG sample is distorted significantly due to vibration-caused positioning errors in the scan trajectory. In contrast, even with a relatively-low (fourth-order) model, the distortions can be reduced by using the optimal-inversion-based feedforward input and the image captures the expected lattice pattern. Thus, Ref. [36] demonstrated that positioning errors can be reduced with the optimal inverse and that the feedforward approach can increase SPM's operating speed.

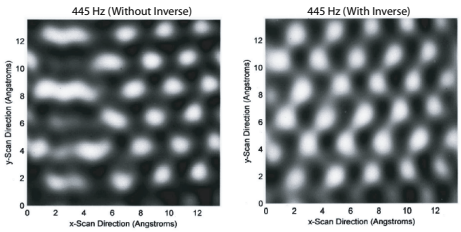

Fig. 4. Comparison of STM images of HOPG surface with (right) and without (left) the optimal inverse input [36].

2.2 Integration with Feedback

Feedforward controllers (which are model based) cannot correct for tracking errors due to plant uncertainties [42]. Therefore, it is necessary to use feedback in conjunction with feedforward to reduce uncertainty-caused errors in the inverse input as shown in Fig. 5. Such an integrated controller was used for piezo-based positioning in, e.g., [43], and demonstrated for SPM control in Ref. [44]. Note that feedback is not the sole workhorse for positioning. Ideally, the feedforward input V_{ff} accomplishes precision positioning $P = P_d$, and the feedback input V_{fb} would be zero. Therefore, feedback design can focus on accounting for the effects of modeling errors and external perturbations.

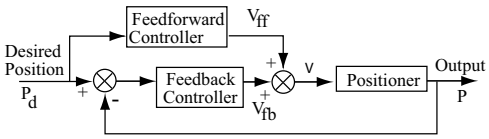

Fig. 5. Augmenting feedback with feedforward.

Remark 4. The addition of feedforward can improve the positioning performance when compared with the use of feedback alone, even in the presence of plant uncertainties. The size of acceptable uncertainties to enable performance improvement with the addition of feedforward has been quantified in [37].

An alternate approach is to use feedback to reduce the uncertainty in the closed-loop system $\mathcal{G}_{\mathcal{CL}}$ as shown in Fig. 6. The closed-loop system $\mathcal{G}_{\mathcal{CL}}$ is used to compute the feedforward input. Thus, the use of feedback can reduce the error in computing the feedforward input. Such an approach to precision positioning was demonstrated for SPM control in Refs. [45]. A simplified computational scheme for finding the feedforward input for such closed-loop piezoscanner dynamics was developed and demonstrated for SPM control in [46].

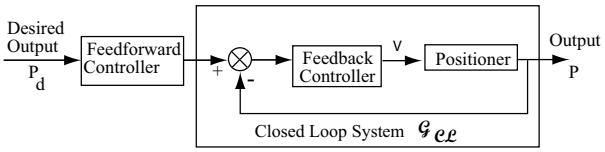

Fig. 6. Inversion-based feedforward of closed-loop system $\mathcal{G}_{\mathcal{CL}}$. The feedback controller reduces the system nonlinearity and uncertainty; the feedforward is the inverse ${\mathcal{G}_{\mathcal{CL}}}^{-1}$ of the linearized closed loop system.

2.3 Handling Nonlinearity

Integration with feedback also facilitates reduction of other effects such as creep and hysteresis. For example, in addition to vibration compensation, creep and hysteresis in the piezoscanner can be also removed by using feedforward techniques as demonstrated in Refs. [47, 48]. The challenge with such feedforward for compensating hysteresis is the modeling complexity. An alternative approach is to reduce the hysteresis effects using feedback — notch filters are used to increase the gain margin of the system and allow the use of higher-gain feedback needed to improve precision [49, 50] as shown in Fig. 7. These notch-filters

can be considered as a *pseudo-inverse* which flattens the frequency response, and thus, increases the gain margin; the notch filters are part of the feedback controller. Experimental results show that this notch-filter approach can lead to a marked increase in the gain margin, and can be used to design feedback controllers that significantly improve the closed loop performance in piezoelectric actuators — even at high frequencies [50]. Therefore, the inversion approach can be applied to the linearized closed-loop system to increase the SPM's operating speed as shown in Ref. [45].

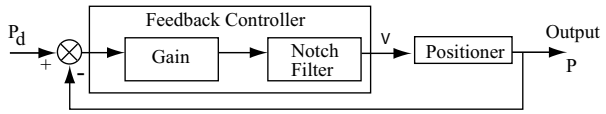

Fig. 7. Use of notch filters in feedback design. This approach can be integrated with either of the feedforward schemes in Figs. 5 or 6.

Alternatively (or additionally), charge control can be used to linearize the nonlinear hysteresis effects before applying the inversion-based approach [51]. For higher-precision SPM applications, the positioning errors due to hysteresis can be reduced further by using an iterative approach as demonstrated in Ref. [52, 53] to increase AFM's operating speed.

2.4 Where to Apply Feedforward?

Figs. 5 and 6 represent two approaches to apply the feedforward. The latter approach, in Fig. 6, reduces the uncertainty in the model used to compute the feedforward. However, the feedforward design is coupled with the feedback design and the achievable positioning bandwidth then depends on the bandwidth of the particular feedback controller. In contrast, the feedforward shown in Fig. 5 does not share the low-gain margin problem of the feedback controller; the computation of the inverse input is decoupled from the feedback design. The drawback is the inability to reduce the modeling uncertainty; this can be alleviated with an iterative correction scheme that is discussed below.

2.5 Improving Feedforward — Iterative Approaches:

Since the positioning application is repetitive (e.g., during periodic scanning of the SPM probe), iterative methods can be used to improve the positioning performance. Therefore, iterative and adaptive control methods are well suited for SPM applications [5]. For example, uncertainty in the inversion process can be reduced using: adaptive inversion of the system model (for both schemes, Fig. 5 and Fig. 6) , see e.g., [54], or learning the *correct* inverse input that yields perfect output tracking, i.e., iterative inversion of the system model, e.g., [55]. The application of such iterative feedforward methods to SPM control was demonstrated in [56]-[58].

3. CURRENT RESEARCH EFFORTS

Two current research efforts in (i) imaging of large soft samples and (ii) image-based control are described below.

3.1 Imaging Large Soft Samples in Liquid

Imaging of cellular features requires SPM imaging with scan dimensions in the range of $20 - 100\mu m$ [59]. For example, the imaging of cell protrusions such as lamellipodia can require scan sizes in the order of $20\mu m$ (see, e.g., Refs. [60, 61]). However, current AFM systems with such large range tend to have imaging time in the minutes. Therefore, current systems are too slow to investigate nano-scale variations in shape and volume of cellular processes with relatively-large features.

Range vs. Speed: High-bandwidth piezoscanners allow increased scan frequencies; however, they also tend to have small scan sizes, i.e., the maximum area that can be imaged is small (e.g., Refs. [9, 32, 34, 62]). For example, the high-speed ($80ms$ per frame) AFM imaging in Ref. [34] had a relatively small scan-area $0.24\mu m \times 0.24\mu m$. An advantage of imaging small samples which facilitates positioning is that the sample profile variation is small and therefore, the vertical changes in SPM-probe position is small. Moreover, during small-area scans the vibrations (due to small lateral motions of the piezoscanner) are also small.

For soft samples, the tradeoff between imaging speed and imaging size is particularly relevant because of the need to maintain small tip-sample forces. While the acceptable tip-sample force depends on the imaging conditions and sample properties, the general trend is a reduction in the imaging speed with an increase in scan size [63]-[68] — as shown in Fig. 8.

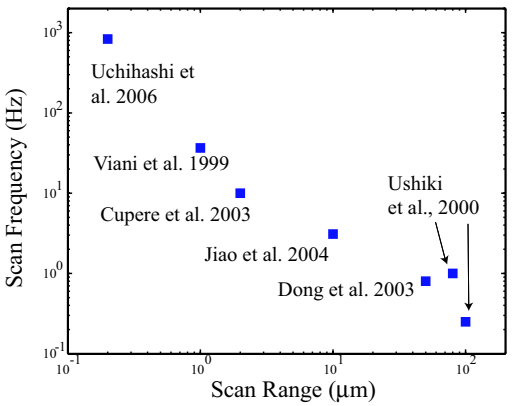

Fig. 8. The tradeoff between scan range and scan frequency (imaging speed) for soft samples in liquid medium [63]-[68].

Recent efforts aim to resolve this conflict, between range and speed, by redesigning the positioner used to move the SPM probe [69, 70]. These redesigns should increase the operating speed of SPMs when imaging large soft samples. It is noted that feedforward methods can improve the performance of such redesigned SPM-probe positioners as well.

Need Feedforward for vertical control: Feedforward for vertical control differs from feedforward for lateral control because the desired vertical position over the sample surface in the vertical direction is unknown before the sample is scanned. In contrast the lateral position is known in advance. The future position is needed to compute

the Fourier transform $P_d(j\omega)$, e.g. in Eq. 4. Therefore, a time domain implementation of the inverses was developed in Ref. [71] for the exact inverse and applied to lateral control for an STM in Ref. [72] using the optimal inverse. However, even in the time domain implementation, some pre-specified amount of preview information of the desired position is needed for precision positioning. Again, preview information of the vertical position is not available in the vertical direction unless the image is scanned in the first place.

Iterative Approach: The iterative control law uses the measured error e_k in the SPM-probe position during one iteration step k to update the current input from one iteration step k to another $k+1$, i.e., from input $V_{ff,k}$ to input $V_{ff,k+1}$, as

$$V_{ff,k+1}(\omega) = V_{ff,k}(\omega) + \rho(\omega)G^{-1}(\omega)\left[E_k(\omega)\right]. \qquad (5)$$

This approach was implemented to STM control using a time-domain implementation of the inversion-based feedforward approach in Ref. [72]. The convergence of such iterative control laws has been studied in [55, 57].

Remark 5. The exact inverse G^{-1} can be replaced with the optimal inverse in Eq. 5.

Problem of Large Forces During First Iteration: The problem is to avoid large tip-sample forces, e.g., during the very first step in the iteration process. At the start of the iteration, the sample profile is unknown; therefore, it is difficult to use the inversion method to achieve the AFM-probe positioning over the sample profile. This can lead to large tip-sample forces and sample damage at the very first iteration. One approach, to avoid such sample damage, is to use a slow scan to identify the sample profile at the start the iteration process and then use the inversion procedure to find the feedforward input. The problem is that this slow scan can take a very long time to begin with and moreover, the sample profile could change during this initial and the images can be distorted by drift effects during slower scans.

Zoom-out/Zoom-in Approach to Reduce Forces: Information from the previous scan line to improve the positioning in the current scan line was developed in Ref. [73]. The main idea is that the current scan profile is close to the previous scan profile and therefore, the positioning can be improved by using the input (for the previous scan line) as a feedforward input in the current scan line. This idea is extended in the zoom-out/zoom-in iterative approach, which has three phases as shown in 9: (i) starting with a small scan area, expand gradually; (ii) fixing the scan size at the desired value, image the sample; and (iii) reduce the scan size to a small value.

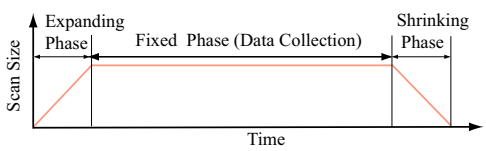

Fig. 9. The three scanning phases (expanding phase, fixed phase, and shrinking phase) to maintain small tip-sample forces during the iteration process. Figure from T. Szuchi

At the start, the scan size is small. Therefore, the sample-profile variations are small; the resulting positioning errors and the tip-sample forces are also small! The rate at which the scan size is changed during the expansion and reduction phases are adjusted to ensure that the variations in the tip-sample force are small. The approach was used to image relatively large soft samples in liquid medium in Refs. [74, 75].

3.2 Image-based Control

Image-based becomes important in subnanometer-scale positioning needed when imaging surfaces at the atomic scale with a Scanning Tunneling Microscope (STM), e.g., when imaging a few carbon atoms in graphite, where the spacing of the atoms is approximately 0.2nm. One of the difficulties in STM control is that external sensors cannot directly measure the position of an STM-probe's atomically sharp tip. Instead they measure the position of a different point on the STM scanner and then infer the position of the STM-probe's tip. Moreover, the resolution of conventional sensors is not sufficient for feedback control of the STM when subnanometer resolution is needed at high speeds (at room temperature) because sensor noise tends to increase with the scan frequency and temperature. This lack of high-resolution measurement capabilities makes the use of feedback control to compensate for dynamic effects in STMs challenging.

To resolve problems with using external sensors, an image-based approach (see Fig. 10) was developed that exploits the extant imaging capability of the STM in [76]. This approach, which uses image-distortions to compensate for dynamic effects, extends previously developed methods that have used STM-images to correct for positioning errors at relatively low operating speeds [77]. The main idea is to quantify the error in positioning the STM-probe's tip over the sample surface by using STM images of standard calibration samples. As the calibration sample surface is fixed, distortions in the image (due to dynamics effects) can be used to quantify the positioning errors and correct the input to the STM. In general samples (rather than calibration samples), topography-feature recognition can be used to correct dynamic effects (e.g., to correct creep effects [78]). Thus, the ability to quantify and correct dynamic effects is only limited by the resolution of the built-in, tunneling-current sensor (of the STM) and not by limitations of external position sensors. Also, because an image-based approach exploits the extant imaging capability of the STM, its use enables an increased operating speed without requiring additional hardware, and therefore, without substantially increasing equipment cost.

An advantage of the image-based approach is that it can be automated using image-distortion-based error estimation algorithms such as those developed in the visual-servoing field, see, for example, [79]. Such automation will make it easy for the end user to not only calibrate, but also recalibrate the STM to account for variations in the scanner dynamics caused by time-varying effects (e.g., aging-related effects) and operating conditions (e.g., temperature). Automation will also allow the image-based approach to be applied to highly parallel micro-fabricated STM systems that are being developed for nanotechnologies. Such miniaturized arrays have higher bandwidth [33]

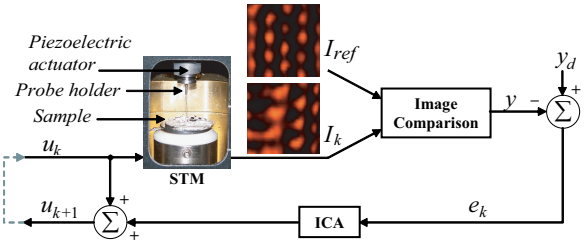

Fig. 10. Image-based STM iterative control [76]. At each iteration step, k, the STM is used to acquire a reference low-speed and a high-speed image (I_{ref} and I_k, respectively). These two images are compared to determine the positioning error e_k, which is used by the iterative control algorithm (ICA) to determine the input u_{k+1} for the next iteration step to improve the STMs positioning accuracy. Image provided by Garrett Clayton.

and increased throughput [18], but their operational speed is still limited by dynamic effects. Thus, higher-speed operation of such miniaturized parallel systems can also be enabled by exploiting the image-based approach.

ACKNOWLEDGEMENTS

This article reviews the results obtained by a number of co-workers including D. Croft, H. Perez, Q. Zou, K. K. Leang, S. Tien, and G. Clayton as mentioned also in the references. The research was funded through NSF grants CMS 0196214, CMS 0336221 and DUE 0632913 as well as NIH grant GM068103.

REFERENCES

[1] G. Binnig and H. Rohrer. Scanning tunneling microscopy. *Helvetica Physica Acta*, 55:726–735, 1982.

[2] G. Binnig, C. F. Quate, and C. Gerber. Atomic force microscope. *Phys. Rev. Lett.*, 56(9):930–933, March, 1986.

[3] L. Pao. A comparison of control architectures for atomic force microscopes. *Keynote paper, Invited Session on Dynamics and Control of Micro- and Nanoscale systems-I, IFAC World Congress*, 2008.

[4] M. V. Salapaka. Systems and control approaches to nano-interrogation: Unraveling new temporal and spatial regimes. *Keynote paper, Invited Session on Dynamics and Control of Micro- and Nanoscale systems-III, IFAC World Congress*, 2008.

[5] S. Devasia, E. Eleftheriou, and R. Moheimani. A survey of control issues in nanopositioning. *IEEE Transactions on Control Systems Technology*, 15(5):802–823, Sept, 2007.

[6] R. Wiesendanger, editor. *Scanning Probe Microscopy and Spectroscopy*. Cambridge University Press, 1994.

[7] S. Alexander, L. Hellemans, O. Marti, J. Schneir, V. Elings, P. K. Hansma, M. Longmire, and J. Gurley. An atomic-resolution atomic-force microscope implemented using an optical lever. *Journal of Applied Physics*, 65(1):164–167, 1989.

[8] M. Gentili, C. Giovannella, and S. Selci, editors. *Nanolithography: A Borderland between STM, EB, IB and X-Ray Lithographies*, volume NATO ASI Series E: Applied Science Vol. 264. Kluwer Academic Publishers, 1993.

[9] R. C. Barrett and C. F. Quate. High-speed, large-scale imaging with the atomic force microscope. *J. of Vacuum Science Technology B.*, 9(2):302–306, 1991.

[10] P. Avouris, T. Hertel, and R. Martel. Atomic force microscope tip-induced local oxidation of silicon: kinetics, mechanism, and nanofabrication. *Appl. Phys. Lett.*, 71:285, 1997.

[11] E. Dubois and J. L. Bubendorff. Kinetics of scanned probe oxidation: Space-charge limited growth. *Journal of Applied Physics*, 87(11):8148–8154, June 2000.

[12] R. Pearce and G. J. Vancso. Real-time imaging of melting and crystallization in poly(ethylene oxide) by atomic force microscopy. *Polymer*, 39(5):1237–1242, March 1998.

[13] L. Li, C.-M. Chan, K. L. Yeung, J.-X. Li, K.-M. Ng, and Yuguo Lei. Direct observation of growth of lamellae and spherulites of a semicrystalline polymer by afm. *Macromolecules*, 34(2):316 – 325, 2001.

[14] L. G. M. Beekmans, D. W. van der Meer, and G. J. Vancso. Crystal melting and its kinetics on poly(ethylene oxide) by in situ atomic force microscopy. *Polymer*, 43(6):1887–1895, March 2002.

[15] S. V. Kalinin and D. A. Bonnell. Effect of phase transition on the surface potential of the $bati0_3$. *Journal of Appl. Phys.*, 87(8):3950–3957, 2000.

[16] E Evans and K Ritchie. Dynamic strength of molecular adhesion bonds. *Biophysical Journal*, 72(4):1541–1555, April, 1997.

[17] B. C. Stipe, M. A. Rezaei, and W. Ho. Single-molecule vibrational spectroscopy. *Science*, 280:1732–1735, 12 June 1998.

[18] K. Wilder, H. T. Soh, A. Atalar, and C. F. Quate. Nanometer-scale patterning and individual current controlled lithography using multiple scanning probes. *Review of Scientific Instruments*, 70:2822–2827, 1999.

[19] S. C. Minne, G. Yaraliuglu, S. R. Manalis, J. D. Adams, J. Zesch, A. Atalar, and C. F. Quate. Automated parallel high-speed atomic force microscopy. *Applied Physics Letters*, 72(18):2240–2342, 1998.

[20] A. L. D. Lozanne, W. F. Smith, and E. E. Ehrichs. Direct writing with a combined stm/sem system. *Proceedings of NATO advanced Workshop on Nanolithography: A Borderland between STM, EB, IB, and X-ray Lithographies*, NATO ASI Series E, Applied Science Vol 264:159–174, 1993.

[21] J. Aizenberg, A.J. Black, and G.M. Whitesides. Control of crystal nucleation by patterned self-assembled monolayers. *Nature*, 398:495–498, 1999.

[22] D. C. Coffey and D. S. Ginger. Patterning phase separation in polymer films with dip-pen nanolithography. *J. Am. Chem. Soc.*, 127:4564, 2005.

[23] S. W. Chung, D. S. Ginger, M. Morales, Z. Zhang, V. Chandrasekhar, M. A. Ratner, and C. A. Mirkin. Top-down meets bottom-up: Dip-pen nanolithography and dna-directed assembly of nanoscale electrical circuits. *Small*, 1:64, 2005.

[24] Cheolmin Park, Jongseung Yoon, and Edwin L. Thomas. Enabling nanotechnology with self assembled block copolymer patterns. *Polymer*, 44(22):6725–6760, Oct. 2003.

[25] Z. Shao, J. Mou, D. M. Czajkowsky, J. Yang, and J-Y Yuan. Biological atomic force microscopy: What is

achieved and what is needed. *Advances in Physics*, 45(1):1–86, 1996.

[26] R. C. Barrett and C. F. Quate. Optical scan-correction system applied to atomic force microscopy. *Rev. Sci. Instrum.*, 62(6):1393–1399, June, 1991.

[27] A. Sebastian and S.M. Salapaka. Design methodologies for robust nano-positioning. *IEEE Transactions on Control Systems Technology*, 13(6):868–876, Nov. 2005.

[28] N. Tamer and M. A. Dahleh. Feedback control of piezoelectric tube scanners. *Proceedings of Control and Decision Conference, Lake Buena Vista, Florida*, pages 1826–1831, 1994.

[29] A. Daniele, S. Salapaka, M.V. Salapaka, and M. Dahleh. Piezoelectric scanners for atomic force microscopes: Design of lateral sensors, indentification and control. In *Proceedings of the American Control Conference*, pages 253–257, San Diego, CA, June 1999.

[30] G. Schitter, P. Menold, H. F. Knapp, F. Allgower, and A. Stemmer. High performance feedback for fast scanning atomic force microscopy. *Rev. Sci. Instrum.*, 72(8):3320–3327, 2001.

[31] S. Salapaka, A. Sebastian, J. P. Cleveland, and M. V. Salapaka. High bandwidth nano-positioner: A robust control approach. *Review of Scientific Instruments*, 73(9):3232–3241, Sept., 2002.

[32] R. Koops and G. A. Sawatzky. New scanning device for scanning tunneling microscope applications. *Rev. Sci. Instrum.*, 63(8):4008–4009, August, 1992.

[33] T. Sulchek, R. Hsieh, J. D. Adams, S. C. Minne, C. F. Quate, and D. M. Adderton. High-speed atomic force microscopy in liquid. *Rev. of Scientific Instruments*, 71(5):2097–2099, May 2000.

[34] T. Ando, N. Kodera, E. Takai, D. Maruyama, K. Saito, and A. Toda. A high-speed atomic force microscope for studying biological macromolecules. *Proceedings of the National Academy of Sciences of the USA*, 98(22):12468–12472, Oct., 2001.

[35] S. John, T. van Noort, K. O. van der Werf, B. G. de Grooth, and J. Greve. High speed atomic force microscopy of biomolecules by image tracking. *Biophysical Journal*, 77:2295–2303, Oct., 1990.

[36] D. Croft and S. Devasia. Vibration compensation for high speed scanning tunneling microscopy. *AIP Rev. Sci. Instrum.*, 70(12):4600–4605, Dec, 1999.

[37] S. Devasia. Should model-based inverse inputs be used as feedforward under plant uncertainty? *IEEE Trans. on Automatic Control*, 47(11):1865–1871, Nov, 2002.

[38] E. Bayo. A finite-element approach to control the end-point motion of a single-link flexible robot. *J. of Robotic Systems*, 4(1):63–75, 1987.

[39] S. Devasia, D. Chen, and B. Paden. Nonlinear inversion-based output tracking. *IEEE Transactions on Automatic Control*, 41(7):930–943, 1996.

[40] J.S. Dewey, K. Leang, and S. Devasia. Experimental and theoretical results in output- trajectory redesign for flexible structures. *ASME Journal of Dynamic Systems, Measurement, and Control*, 120(4):456–461, December, 1998.

[41] R. Brinkerhoff and S. Devasia. Output tracking for actuator deficient/redundant systems: Multiple piezoactuator example. *AIAA J. of Guidance, Control, and Dynamics*, 23(2):370–373, March-April 2000.

[42] Y. Zhao and S. Jayasuriya. Feedforward controllers and tracking accuracy in the presence of plant uncertainties. *ASME Journal of Dynamic Systems, Measurement, and Control*, 117:490–495, December,1995.

[43] D. Croft, S. Stilson, and S. Devasia. Optimal tracking of piezo-based nano-positioners. *J. of Nanotechnology*, 10:201–208, June 1999.

[44] Q. Zou, K. K. Leang, E. Sadoun, M. J. Reed, and S. Devasia. Control issues in high-speed afm for biological applications: Collagen imaging example. *Special Issue on* Advances in Nano-technology Control, *Asian Journal Control*, 6(2):164–178, June 2004.

[45] K. K. Leang and S. Devasia. Feedback-linearized inverse feedforward for creep, hysteresis, and vibration compensation in afm piezoactuators. *IEEE Transactions on Control Systems Technology*, 15(5):927–935, September, 2007.

[46] Yang Li and John Bechhoefer. Feedforward control of a closed-loop piezoelectric translation stage for atomic force microscope. *Review of Scientific Instruments*, 78, 013702:1–8, January, 2007.

[47] D. Croft and S. Devasia. Hysteresis and vibration compensation for piezo actuators. *AIAA Journal of Guidance, Control and Dynamics*, 21(5):710–717, September-October, 1998.

[48] D. Croft, G. Shedd, and S. Devasia. Creep, hysteresis, and vibration compensation for piezoactuators: Atomic force microscopy application. *ASME Journal of Dynamic Systems, Measurement and Control*, 123(35):35–43, March, 2001.

[49] Y. Okazaki. A micro-positioning tool post using a piezoelectric actuator for diamond turning machines. *Precision Engineering*, 12:151–156, July 1990.

[50] K. Leang and S. Devasia. Hysteresis, creep, and vibration compensation for piezoactuators: Feedback and feedforward control. *Proceedings of 2nd IFAC Conference on Mechatronic Systems, Berkeley, CA*, pages 283–289, Dec 9-11, 2002.

[51] G. M. Clayton, S. Tien, A. J. Fleming, S. O. R. Moheimani, and S. Devasia. Inverse feedforward of charge controlled piezopositioners. *Accepted to Mechatronics*, To Appear, 2007.

[52] K. K. Leang and S. Devasia. Design of hysteresis-compensating iterative learning control: Application to atomic force microscopes. *Mechatronics*, 16(3-4):141–158, April-May, 2006.

[53] Ying Wu and Qingze Zou. Iterative control approach to compensate for both the hysteresis and the dynamics effects of piezo actuators. *IEEE Transactions on Control Systems Technology*, 15(5):936–944, September, 2007.

[54] T. Tsao and M. Tomizuka. Adaptive zero phase error tracking algorithm for digital control. *ASME Journal of Dynamic Systems, Measurement, and Control*, 109(2):349–354, December, 1987.

[55] J. Ghosh and B. Paden. A pseudo-inverse based iterative learning control. *IEEE Trans. on Automatic Control*, 47(5):831–837, May,2002.

[56] G. Schitter, R. W. Stark, and A. Stemmer. Fast contact-mode atomic force microscopy on biological specimen by model-based control. *ULTRAMI-*

CROSCOPY, 100(3-4):253–257, Aug, 2004.

[57] S. Tien, Q. Zou, and S. Devasia. Iterative control of dynamics-coupling-caused errors in piezoscanners during high-speed afm operation. *IEEE Transactions on Control Systems Technology*, 13(6):921–931, Nov 2005.

[58] G. M. Clayton and S. Devasia. Iterative image-based modeling and control for higher scanning probe microscope performance. *Review of Scientific Instruments*, 78(8):Article No. 083704 (pp. 1–12, August 29, 2007.

[59] P. P. Lehenkari, G. T. Charras, A. Nykanen, and M. A. Horton. Adapting atomic force microscopy for cell biology. *Ultramicroscopy*, 82:289–295, 2000.

[60] V C Abraham, V Krishnamurthi, D L Taylor, and F Lanni. The actin-based nanomachine at the leading edge of migrating cells. *Biophysical Journal*, 77(3):1721–1732, Sept., 1999.

[61] J. V. Small, T. Stradal, E. Vignal, and K. Rottner. The lamellipodium: where motility begins. *Trends in Cell Biology*, 12(3):112–120, March, 2002.

[62] M B Viani, L I Pietrasanta, J B Thompson, A Chand, I C Gebeshuber, J H Kindt, M Richter, H G Hansma, and P K Hansma. Probing protein-protein interactions in real time. *Nature Structural Biology*, 7(8):644–647, 2000.

[63] T. Uchihashi, T. Ando, and H. Yamashita. Fast phase imaging in liquids using a rapid scan atomic force microscope. *Applied Physics Letters*, 89(213112):1–3, November, 2006.

[64] H. Dong, M. Wanyun, L. Fulong, Y. Meiling, O. Zhigang, and S. Yunxu. Time-series observation of the spreading out of microvessel endothelial cells with atomic force microscopy. *Physics in Medicine and Biology*, 48:3897–3909, 2003.

[65] T. Ushiki, S. Yamamoto, J. Hitomi, S. Ogura, T. Umemoto, and M. Shigeno. Atomic force microscopy of living cells. *Japanese Journal of Applied Physics*, 39(6B):3761–3764, June, 2000.

[66] M. B. Viani, T. E. Schäffer, G. T. Paloczi, L. I. Pietrasanta, B. L. Smith, J. B. Thompson, M. Rief, H. E. Gaub, K. W. Plaxco, A. N. Cleland, H. G. Hansma, and P. K. Hansma. Fast imaging and fast force spectroscopy of single biopolymers with a new atomic force microscope designed for small cantilever. *Review of Scientific Instruments*, 70(11):4300–4303, 1999.

[67] Y. Jiao and T. E. Schäffer. Accurate height and volume measurements on soft samples with the atomic force microscope. *Langmuir*, 20:10038–10045, 2004.

[68] V. M. D. Cupere, J. V. Wetter, and P. G. Rouxhet. Nanoscale organization of collagen and mixed collagen-pluronic adsorbed layers. *Langmuir*, 19:6957–6967, 2003.

[69] G. Schitter, K. J. strm, B. E. DeMartini, P. J. Thurner, K. L. Turner, and P. K. Hansma. Design and modeling of a high-speed afm-scanner. *IEEE Transactions on Control Systems Technology*, 15(5):906–915, September, 2007.

[70] Y. Ando, T. Ikehara, and S. Matsumoto. Development of three-dimensional microstages using inclined deep-reactive ion etching. *JOURNAL OF MICRO-ELECTROMECHANICAL SYSTEMS,*, 16(3):748–751, June, 2007.

[71] Q. Zou and S. Devasia. Preview-based stable-inversion for output tracking. *ASME J. of Dynamic Systems, Measurement and Control*, 121(4):625–630, Dec, 1999.

[72] Q. Zou and S. Devasia. Preview-based optimal inversion for output tracking: Application to scanning tunneling microscopy. *IEEE Transactions on Control Systems Technology*, 12(3):375–386, May, 2004.

[73] G. Schitter, F. Allgöwer, and A. Stemmer. A new control strategy for high-speed atomic force microscopy. *Nanotechnology*, 15:108–114, 2004.

[74] Szuchi Tien. High-speed nano-precision positioning: Theory and application to afm imaging of soft samples. *Ph.D Thesis, U. of Washington, Seattle*, July 2007.

[75] Szuchi Tienand S. Devasia. Afm imaging of large soft samples in liquid medium using iterative inverse feedforward control. *American Control Conference*, Submitted in 2007.

[76] G. Clayton and S. Devasia. Image-based control of dynamic effects in scanning tunneling microscopes. *Nanotechnology*, 16(6):809–818, June 2005.

[77] R. V. Lapshin. Automatic lateral calibration of tunneling microscope scanners. *Review of Scientific Instruments*, 69(9):3268–76, Sept., 1998.

[78] R. V. Lapshin. Automatic drift elimination in probe microscope images based on techniques of counter-scanning and topography feature recognition. *Measurement Science and Technology*, 18(3):907–927, March, 2007.

[79] S. Hutchinson, G. Hager, and P. Corke. A tutorial on visual servo control. *IEEE Trans. Robotics Automation*, 12:651–670, Oct. 1996.